3.2

TOTAL LIGHTNING AS AN INDICATION OF CONVECTIVELY INDUCED TURBULENCE POTENTIAL IN AND AROUND THUNDERSTORMS

Ryan Rogers*[1], Lawrence Carey[1], Kris Bedka[2], Wayne Feltz[3], Monte Bateman[4], Geoffrey Stano[5]
[1] Atmospheric Science Department, University of Alabama-Huntsville
[2] SSAI/NASA LaRC
[3] CIMSS, University of Wisconsin-Madison
[4] USRA, Huntsville, Alabama
[5] NASA SPoRT, Huntsville, Alabama

1. INTRODUCTION

Thunderstorms and their associated hazards pose a serious risk to general, commercial, and military aviation interests. The threat to aircraft from thunderstorms primarily manifests itself in three areas: icing, lightning, and turbulence. These hazards can be mitigated by avoiding thunderstorms by as wide a margin as is possible. With aviation hazard reduction in mind, the Federal Aviation Administration (FAA) provides some guidelines for pilots to follow to maintain a safe distance from thunderstorms in their 2012 publication of the Aeronautical Information Manual (AIM) in section 7-1-29 dealing with thunderstorm flying. A few particularly relevant rules are:

1. Do avoid by at least 20 nautical miles any thunderstorm identified as severe or giving an intense radar echo. This is especially true under the anvil of a large cumulonimbus.

2. Do clear the top of a known or suspected severe thunderstorm by at least 1000 feet altitude for each 10 knots of wind speed at the cloud top. This should exceed the altitude capability of most aircraft.

3. Do circumnavigate the entire area if the area has 6/10 thunderstorm coverage.

Adherence to these guidelines can render large areas of airspace unusable in particularly busy convective environments and in especially congested airspace. Therefore, it is not always practical or possible to explicitly follow the FAA guidelines but the fact remains that direct and indirect effects from thunderstorms are responsible for significant numbers of injuries and monetary losses to the aviation industry as a whole. Weber et al. (2006) analyzed FAA statistics and found that thunderstorm related flight delays cost the commercial aviation industry approximately 2 billion dollars annually in direct operating expenses. All threats to aviation associated with thunderstorms are a result of the kinetic energy contained in the thunderstorm updraft. Just the presence of lightning within a convective cell gives some indication as to the strength of the updraft. Total Lightning (IC+CG) information can reveal not only the location of the convective updraft but can also give clues as to the strength of the convection. Thunderstorms, by definition, contain lightning and the ability to detect and interpret lightning information is a valuable tool to determine which air space has increased potential for Convectively Induced Turbulence (CIT), particularly in regions where radar coverage is sparse or lacking altogether. It is hoped that the findings of this research will be applicable to data received from the Geostationary Lightning Mapper (GLM) on board the next generation GOES-R satellite scheduled for launch in early 2016. The GLM will allow total lightning detection capability across most of the western hemisphere at roughly 8 km^2 resolution from geostationary orbit

**Corresponding author address:* Ryan H. Rogers, Earth System Science Center, UAHuntsville, 320 Sparkman Drive, Huntsville, AL 35805; e-mail: rogersr@nsstc.uah.edu

2. BACKGROUND

Convectively induced turbulence (CIT) is an aviation term encompassing all convectively induced turbulent motions that cause a turbulent response in aircraft (Lane et al. 2003). Cornman and Carmichael (1993) found that CIT may account for over 60% of turbulence encounters over the United States. Additionally, CIT events tend to be highly transient in both space and time (Hamilton and Proctor 2002; Lane et al. 2003) making them especially difficult to track and forecast. Kaplan et al. (2004) studied the meteorological conditions present in 44 severe, accident-producing turbulence encounters and found that well over 80% of the cases they studied occurred within 100 km of moist convection. It follows that decreases in the distance between aircraft and convective updrafts should result in greater chances for CIT as has been found in numerous other studies (e.g. Bedka et al. 2010; Lane et al. 2012). In fact, Lane et al. (2012) state that, "the risk of moderate or greater (MOG) turbulence is almost twice the background value as far as 70 km from the storm".

A common framework is necessary to define turbulence magnitude with values ranging from light turbulence at the low end to extreme turbulence at the high end. Pilot reports (PIREPs) have been the traditional means of quantifying the turbulence found in and around thunderstorms. Unfortunately, PIREPs are dependent on the pilot's subjective assessment of turbulence magnitude as well as the specific response characteristics of the particular aircraft. In addition, the pilot must radio his or her observations to the ground, which can result in significant temporal and spatial deviations from the precise location where the turbulence was encountered. These factors render PIREP data less than ideal for research applications. Cornman et al. (1995) outlined a way in which many of the drawbacks of the PIREP system could be eliminated and result in a research-quality metric of aviation turbulence that is suitable for verification of forecasts and algorithms. The Eddy Dissipation Rate (EDR) is calculated using existing sensors, avionics, and communication technology to produce and disseminate an objective, aircraft independent, state-of-the-atmosphere turbulence metric (Cornman et al. 1995). These objective measures of turbulence are now available on a significant number of aircraft using the FAA's automated turbulence reporting system and the National Center for Atmospheric Research (NCAR) in-situ algorithms. Eddy dissipation rates are calculated and reported every minute regardless of meteorological conditions or pilot/ground support staff workload and thus EDR data offer a significant improvement over PIREP-derived turbulence data.

Numerous studies have shown that there are useful correlations between trends in lightning characteristics and thunderstorm strength (e.g. Goodman 1988; Steiger et al. 2007; Schultz et al. 2011). Recent work has also shown that total lightning is a much more complete indicator of thunderstorm strength than CG data alone, since increases in updraft strength and resultant microphysical modifications are first manifested electrically in the form of increases in the IC flash rate, which is a component of total lightning (e.g. Williams et al. 1999; Wiens et al. 2005). Findings of this nature indicate that changes in updraft characteristics will manifest themselves in changes in the total lightning flash rate and these changes can be used to assess the strength of the updraft and, by extension, the potential for CIT.

3. DATA

The present study necessarily involves the exploration and manipulation of a wide range of meteorological and aviation information including lightning, radar, and turbulence datasets. Radar data for this study comes from the National Weather Service's Weather Surveillance Radar-1988 Doppler (WSR-88D) network and includes radar reflectivity as well as Vertically Integrated Liquid (VIL).

Total lightning data were primarily observed with the North Alabama Lightning Mapping Array (NALMA) which has been operated by NASA continuously since 2001 (Goodman et al. 2005). The NALMA is a 3 dimensional Very High Frequency (VHF) Time of Arrival (TOA) network consisting of 11 sensors dispersed across northern Alabama with a base station located at the National Space Science and Technology Center (NSSTC) on the campus of the University of Alabama in Huntsville. Typical location errors within 150 km of the network center are on the order of 50 m in the horizontal and 100 m in the vertical, with location errors increasing with the square of the range from network center at distances greater than ~150 km (Koshak et al. 2004). While overall in-network flash detection efficiency is excellent, the aforementioned location errors, line of sight issues and general decrease in sensitivity at large ranges can result in degradation of detection efficiency (Rison et al. 1999). For these reasons the current study will only examine lightning flashes that initiated within 150 km of the NALMA network center. Additionally, we utilized the flash clustering algorithm detailed in McCaul et al. (2005; 2009) to group individual radiation sources into coherent flashes. For the purposes of this study we selected only those flashes with 8 or more sources per flash for inclusion in the analysis.

In order to test the findings in this study at GLM resolution we have utilized data from the GLM proxy (Bateman et al. 2008). This product utilizes a combination of LMA and Lightning Imaging Sensor (LIS) lightning data in order to make a statistical best guess as to what the GLM will detect when launched. The GLM proxy algorithm matches LMA source data with a database of prior LIS flashes to produce estimates of flash characteristics at 8 km^2 resolution. In cases where both the NALMA and the LIS detected flashes at the same time and place it was found that only LMA flashes with 30 or more sources routinely registered on the LIS (Proch 2010). GLM proxy data will likely differ from native LMA data in overall flash count and rate due to the more stringent source per flash criteria and can differ in spatial location as a result of coarser 8 km^2 resolution of the GLM proxy.

In addition to NALMA VHF data, this study also examines data from the Earth Networks Total Lightning Network (ENTLN) in order to compare the two networks. ENTLN is a ground-based TOA detection network consisting of over 700 sensors that continuously detect lightning in the 1 Hz-12MHz range (ENTLN 2012). This exceptionally wide frequency range permits the detection of both IC and CG lightning (Liu and Heckman 2010). ENTLN is a relatively new network with most sensors coming online in 2010 and expanding further thereafter. In areas of high sensor density, ENTLN has total lightning detection capability but in areas with low sensor density the network favors the detection of CG flashes (Thompson 2013). Receiving stations capture and record complete wave forms and transmit them to the central processing station where Earth Networks claims that this rich signal information allows for estimation of peak current and excellent purported detection efficiency, with up to 95% of ICs detected in some sensor-dense areas (Liu and Heckman, 2010). In Northern Alabama, Thompson (2013) found that relative flash detection efficiency compared to LIS was approximately 60% to 80% for total lightning. For this study we used internally quality controlled data from ENTLN and implemented a flash clustering scheme, similar to what is outlined by Cummins et al. (1998) for National Lightning Detection Network (NLDN) data, which determines flashes by subjecting raw stroke and pulse information to temporal and spatial constraints. Flash data from ENTLN will be included for comparison with NALMA and GLM proxy data in a few specific plots.

Peak EDR data were obtained from NCAR for 2010 and 2011. Only flights experiencing moderate or greater (MOG) EDR turbulence within 150 km of the center of the NALMA were considered in order to maximize the location accuracy and detection efficiency of LMA data. In addition, some further quality control measures were applied to the EDR data to minimize erroneous turbulence reports that may have resulted due to deliberate, controlled changes in aircraft altitude. These additional measures exclude the following types of data:

1. All EDR reports from below 20,000 ft.

2. All EDR reports that were determined to be from either ascending or descending legs of a flight (flagged and removed if total ascent or descent was greater than 5000 ft over 15 minutes), and EDRs which indicate a change in altitude of greater than 333 ft min^{-1}.

The vast majority of flights that met the above criteria were associated with flights operated by Delta Airlines. Delta has its main hub at the Atlanta Hartsfield Jackson International Airport and flights to and from this hub make up the vast majority of EDR-reporting flights in the Alabama region during the 2010-2011 period. Due to the close proximity of Huntsville and Atlanta there are some flights that appear to begin or stop reporting abruptly, this is a symptom of the aforementioned EDR altitude quality control measures as aircraft begin descent to or complete ascent from Atlanta airspace. Peak EDR data are normalized to values between 0.05 and 0.95 (in 0.1 increments) and are preferable to median EDR values because they provide a good indication of the hazard to aircraft and are better distributed over the turbulence severity reporting bins (Lane et al. 2012). There is conflicting information on exactly what EDR values correspond to which level of turbulence (light, moderate, severe). Since these descriptors were designed for use with subjective, aircraft dependent PIREP data it may not always be beneficial or consistent to assign these descriptors to EDR turbulence information. However, for this study we will follow the convention recommended by Sharman and Williams (personal communication, 2013) which is also used in Bedka et al. (2010) and shown in Table 1**.**

Table 1: EDR turbulence category and magnitude.

Turbulence	EDR Range
None	EDR ≤ 0.05
Light	0.05 < EDR ≤ 0.25
Moderate	0.25 < EDR ≤ 0.45
Severe	EDR > 0.45

4. Methodology

The approach employed in this study differs from other experiments that track the location, strength, and trends of individual or associated convective cells. Instead, this study seeks to examine the total lightning properties that occur around the EDR-reporting aircraft in an attempt to quantify the convective turbulence threats. This aircraft-centric, Lagrangian approach highlights the conditions in the aircraft's vicinity on flights in which MOG turbulence was experienced. In the course of conducting related research it was observed that aircraft were close, and in some cases extremely close, to radar and total lightning indicated convective cores. As previously mentioned, the FAA provides guidelines for aircraft to follow while in the vicinity of active convection. These are guidelines and not hard-and-fast rules that are required to be followed. That being said, it appears that these guidelines were often not heeded and resulted in turbulence that could have otherwise been avoided had the FAA recommendations been adhered to more strictly. Utilization of lightning flash initiation location information is an excellent method with which to assess the separation between aircraft and convective threats.

The inclusion of EDR data has provided a unique opportunity to examine how convective metrics change while an aircraft is in close proximity to convection. Every minute, EDR data provide spatial information on aircraft location in addition to turbulence magnitude. The aircraft time and space information included in EDR data allow for the calculation of the distance between the aircraft and lightning features in order to explore the relationship between observed turbulence and proximity to convective updrafts.

The FAA recommends a 20 nautical mile horizontal separation between aircraft and suspected strong convection. For this study we have examined the lightning properties that fall within this moving horizontal buffer zone. There are many varied aspects of LMA data that can be examined to diagnose the threat posed by thunderstorms, including: source location information, flash initiation locations, flash rate, and trends in flash rate. The mere presence of lightning gives some indication as to the depth, strength, and turbulence potential of convection (Deierling and Petersen 2008). The updraft is the key to both lightning and turbulence generation and as such any lightning properties that highlight the location and intensity of the updraft are particularly well suited for use in this study. To this end, this study has primarily examined the spatial distribution of LMA flash initiations and flash rates since flashes typically begin in areas of strong electric fields between major charge reservoirs and can therefore be used as an analog for updraft location. The distance from aircraft to individual LMA sources was also considered for further analysis but since a number of our cases feature spatially extensive MCSs that are known to contain flashes of extreme horizontal extent it is believed that the distance from the aircraft to an LMA source location will not always provide a good estimate of updraft location. In addition to the LMA variables listed above we have examined the related GLM proxy initiation location and flash rate data at 8 km^2 resolution to quantify how changes in resolution might affect these results.

Utilization of EDR data has also provided a unique opportunity to examine lightning characteristics at positions where the aircraft will be in the future. In this way we can assess the lightning characteristics at future positions to test whether there is any predictive capability to these lightning data by measuring them against the turbulence experienced by the aircraft when it reaches these positions. Both the total number of accumulated flashes and distance to flash initiations are examined ahead of the aircraft to gauge any potential predictive signals which may indicate turbulence.

5. RESULTS

Details from three representative flights that experienced MOG turbulence within 150 km of the NALMA are examined. These cases were chosen to show results from varying season as well as a variety of convective morphologies. Plots showing the aircraft position, the recommended horizontal buffer of 20 nmi, and color coded turbulence magnitude are overlaid on low level radar reflectivity with LMA flash initiations to illustrate aircraft proximity to radar and lightning indicated features. Plots showing the flash rate from NALMA, GLM proxy, and ENTLN are shown to highlight variation in results from the various total lightning products. Flash initiation density is overlaid on WSR-88D VIL along with the approximate track of the aircraft in an attempt to emulate the look and feel of GLM resolution flash initiation density. Finally, plots examining the flash rate and distance to nearest flash initiation are shown for each location that the aircraft registered an EDR report regardless of the aircraft's position. In this way we can examine the lightning intensity and distance information at future aircraft positions for value in CIT prediction.

a. January 24th, 2010 Delta Flight 2007

This flight provides a particularly informative research case as it illustrates total lightning data's ability to highlight which convective regions are more susceptible to increased turbulence risk in a low flash rate environment. This day was characterized by a very weak thermodynamic forcing for strong convection resulting in very few lightning flashes across the NALMA domain. This particular flight was the only MOG flight of the day that had lightning within 20 nmi of the aircraft. Of note in Figure 1 is the single **+,** indicating an LMA flash initiation, between the two yellow moderate turbulence diamonds. This particular cell had a history of producing lightning flashes in the minutes leading up to the moderate turbulence reports. The simple fact that this particular cell was strong enough to produce lightning serves to differentiate it from other cells in the region when radar reflectivity shows little indication that this cell is any more robust than others in the vicinity.

Flash rates were computed using a variety of networks and are detailed in Figure 2. The NALMA and ENTLN detect flashes at the same times for this case but interestingly, ENTLN flash rate is double what was detected by the NALMA for this case (peak of 4 and 2 flashes per minute respectively). This discrepancy could be a result of the 8 source per flash criteria imposed on NALMA flashes. Also of note in Figure 2 is the total lack of GLM proxy flashes, which is likely the result of the much more stringent 30 sources per flash requirement for this product.

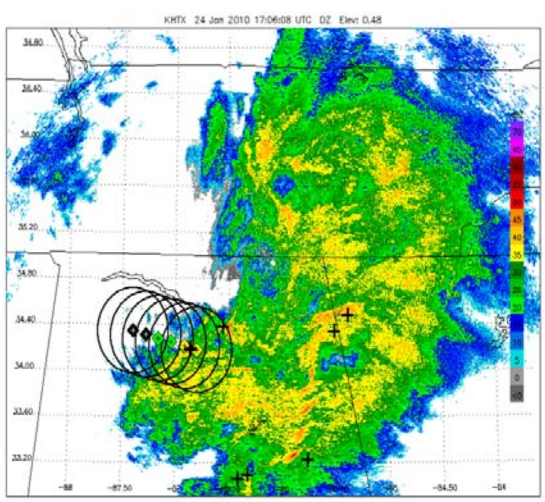

Figure 1: Low level reflectivity from KHTX, LMA flash initiations from the 6 minutes centered on the radar scan time ('+' symbols), 20 nmi aircraft radius (circle), and color-coded aircraft location turbulence magnitude.

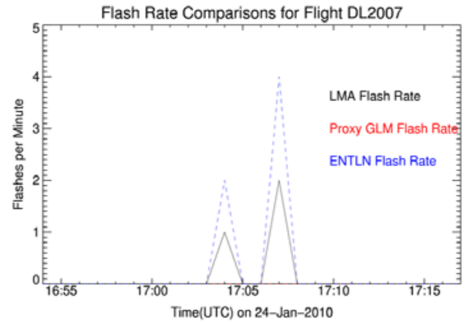

Figure 2: Flash rates from different lightning products; with LMA in solid black, GLM-proxy in dotted red, and ENTLN in dotted blue for DL2007.

Figure 3 shows coarse resolution flash initiation density plotted overtop of WSR-88D VIL with the aircraft track in red. Flash initiation density gives a good approximation for updraft location and plots of a similar nature could be useful after the launch of GOES-R/GLM. Figures 4 and 5 examine the prevalence and characteristics of lightning at each EDR position of DL2007 even when the aircraft is not necessarily occupying that position. Figure 4 shows the total number of flashes that were initiated within 20 nmi of each position over the entire flight duration. This plot indicates which locations experienced the most lightning during the time the aircraft was traversing the area. It is clear from the figure that the area with the most flashes (positions 11-15; all with at least 6 accumulated flashes) is largely collocated with the area in which the aircraft experienced the greatest turbulence, registering an EDR value above 0.4 at position 13. In addition, Figure 5 outlines the result when the minimum distance from each position to these flashes is calculated. There is a clear minimum in this distance to flash initiations at positions 12 and 13, with corresponding minimum distances of roughly 3 nmi, that is coincident with the greatest turbulence. So, not only were these locations experiencing the most lightning but they were also the positions that were closest to the lightning initiations. Results of the type shown in Figures 4 and 5 could be extremely useful in defining exactly which areas are the most likely to feature the greatest turbulence given a lack of indications from radar observations.

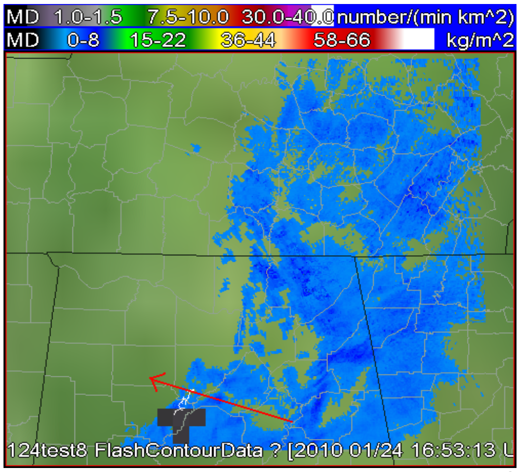

Figure 3: Flash initiation density (black squares), flash contours, WSR-88D VIL and aircraft track (red).

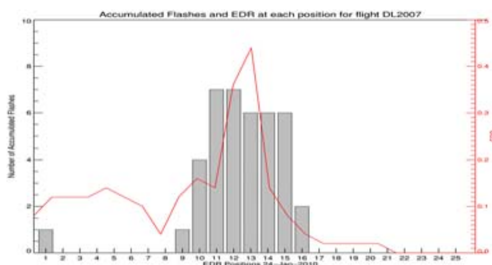

Figure 4: Accumulated flashes at each EDR report position for the duration of DL2007 (bars) and aircraft EDR turbulence (red).

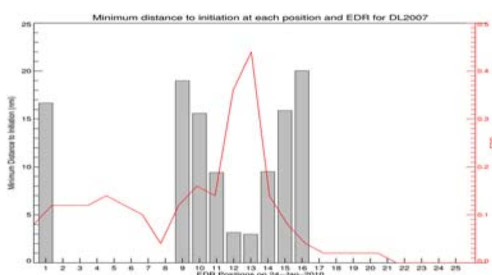

Figure 5: Minimum distance to LMA flash initiations (bars) at each position for the duration of DL2007 and aircraft EDR turbulence (red) measured along flight path.

b. March 12th, 2010 Delta Flight 1511

Flight 1511 is an example of a horizontally extensive convective system characterized by robust flash rates that forced pilots and airline dispatchers to try and find safe gaps between strong convective cells. Aircraft deviation around this area of convection would likely have resulted in significant costs in time and fuel. Figure 6 shows that there does indeed appear to be a gap between stronger convective elements associated with elevated reflectivity. From a purely radar perspective it would seem that the gap navigated by DL1511 was the best option. Examination of data from the LMA in Figure 6, however, does indicate that there were multiple lightning initiations in the gap for which this flight was heading. Consideration of these data could have highlighted the turbulence threat in this area.

Examination of the flash rates found by different lightning products in Figure 7 shows results similar to what has been found in the previous case with a few minor exceptions. All total lightning products show coincident peaks in flash rate at 12:09 UTC with the native NALMA data detecting 16 flashes per minute, followed closely by GLM proxy with 15 flashes per minute, and finally ENTLN with 10 flashes per minute. Given the extensive convection on this day the aforementioned reasons for variation in lightning products still apply. The close agreement between LMA and GLM proxy flash rates attest to the fact that flashes in the vicinity of the aircraft likely included a relatively large number of sources. This agreement can also help to explain the relative reduction in ENTLN flash rates since flashes with large numbers of sources are not excluded by the LMA minimum source criteria. Convection featuring relatively few sources per flash should tend to inflate ENTLN flash counts with respect to flash counts from LMA data, as was likely the case with the previous case example.

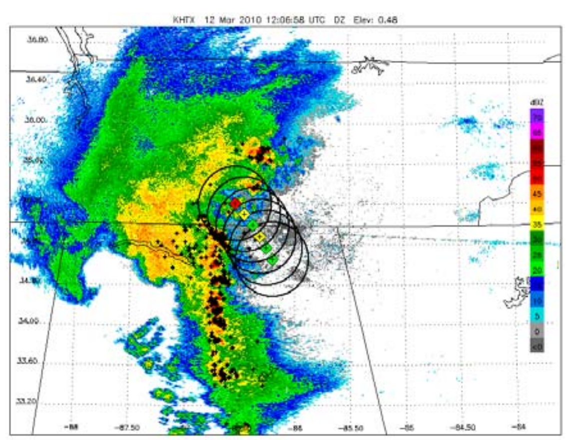

Figure 6: Low level reflectivity from KHTX, LMA flash initiations from the 6 minutes centered on the radar scan time ('+' symbols), 20 nmi aircraft radius (circle), and color-coded aircraft location turbulence magnitude.

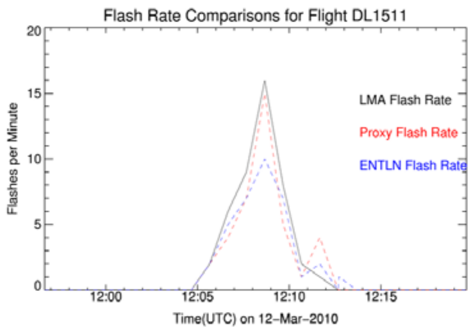

Figure 7: Flash rates from different lightning products; with LMA in solid black, GLM-proxy in dotted red, and ENTLN in dotted blue for DL1511.

Figure 8 again shows the coarse resolution flash initiation density overlaid on radar VIL with the approximate aircraft track shown in red. Even at this coarse resolution it is apparent that the gap as indicated by radar is not as benign from a lightning perspective as it is from the radar perspective. Figures 9 and 10 examine the lightning characteristics at positions in which the aircraft reported EDR data. The accumulated flash data in Figure 9 clearly highlights the positions with the most lightning over the course of the flight and these data correspond closely with the peak in turbulence experienced by DL1511. Nearly 300 flashes initiated at position 14 during the course of DL1511 which was adjacent to the position in which the flight experienced severe turbulence. Examination of the minimum distance to flashes data contained in Figure 10 show that, in general, the greatest turbulence was experienced in positions with relatively short minimum distances to flash initiations. The locations with EDR above 0.30 (positions 12, 14, 15, and 16) all have minimum distances to flash of 7 nmi or less and nearly every position recorded at least one flash that initiated within 20 nmi. Data of the sort shown in Figures 9 and 10 could be very useful in helping to determine exactly which areas in the flight path have increased threat from turbulence.

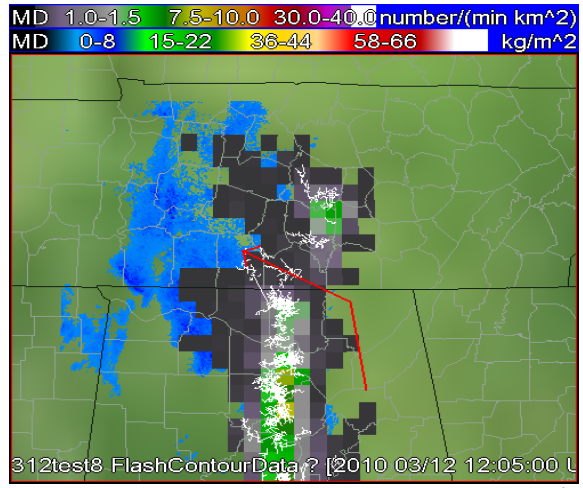

Figure 8: Flash initiation density (black squares), flash contours, WSR-88D VIL and aircraft track (red).

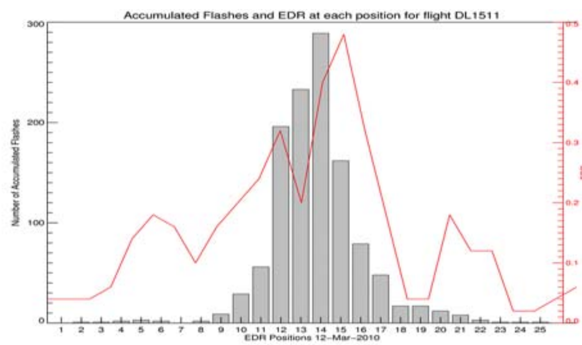

Figure 9: Accumulated flashes at each EDR report position for the duration of DL1511 (bars) and aircraft EDR turbulence (red).

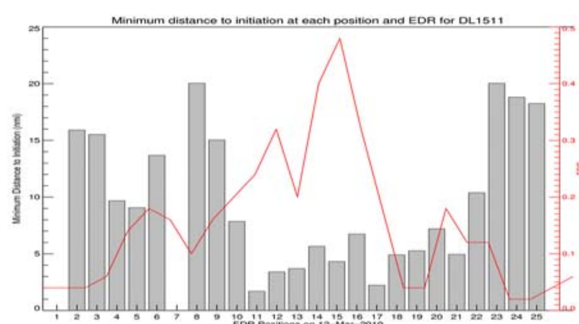

Figure 10: Minimum distance to LMA flash initiations (bars) at each position for the duration of DL1511 and aircraft EDR turbulence (red) measured along flight path.

c. June 1st, 2010 Delta Flight 0724

This case day was characterized by widely scattered and weakly forced convection in contrast to the previous 2 cases detailed above. The availability of deviation options around these widely spaced convective cells is much more apparent than in the previous cases. DL0724 experienced moderate turbulence shortly after flying over a small, lightning producing cell. The flight was also within 20 nmi of another strongly flashing cell to its north as can be seen in Figure 11. Several flights in the time preceding DL0724 (not shown) traveled very close to the stronger northern cell and did not register any turbulence suggesting that the turbulence experienced by DL0724 was associated with the small overflown cell. FAA guidelines recommend not flying over developing convection unless the aircraft can be 1000 ft above the cloud for each 10 kts of wind speed at cloud top. Examination of EDR altitude data and KHTX WSR-88D echo top height indicate that DL0724 was, in fact, less than 1000ft above the radar indicated top of the small cell with environmental winds of roughly 20 kts at that level. Figure 11 illustrates the widely scattered nature of the convection on this day which suggests that deviation around convective cells was likely not prohibitively costly with respect to time or money. Figure 11 also shows a different EDR instrumented flight that appears to be heading directly into another convective cell near the Alabama-Georgia border when multiple deviation options are available for this flight as well.

Figure 12 illustrates the lightning characteristics around DL0724 as found by the different lightning products. The ongoing theme of similar trends but varying magnitudes between networks is again apparent in this figure with the GLM proxy detecting 11 flashes per minute in contrast with 9 flashes per minute and 3 flashes per minute from LMA and ENTLN, respectively. Variations in resolution are responsible for the variation between GLM proxy and native LMA while variations in detection efficiency between LMA and ENTLN are a likely explanation for the discrepancy between LMA and ENTLN flash rates.

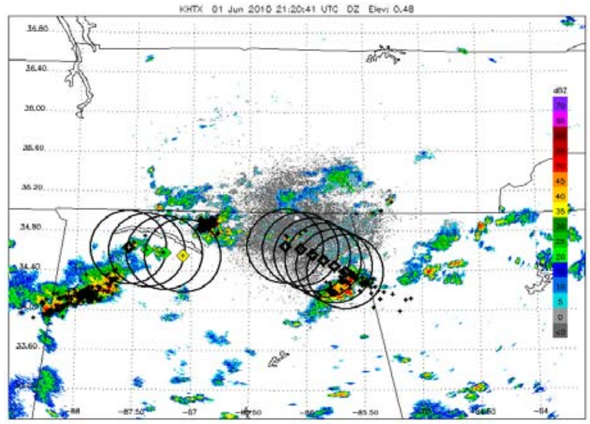

Figure 11: Low level reflectivity from KHTX, LMA flash initiations from the 6 minutes centered on the radar scan time ('+' symbols), 20 nmi aircraft radius (circle), and color-coded aircraft location turbulence magnitude.

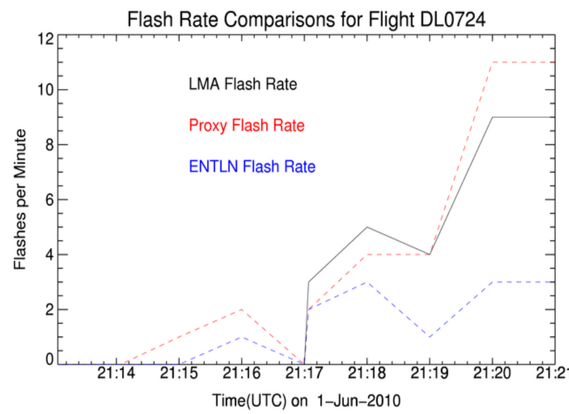

Figure 12: Flash rates from different lightning products; with LMA in solid black, GLM-proxy in dotted red, and ENTLN in dotted blue for DL0724.

Figure 13 shows the flash initiation density and radar VIL along with the aircraft track in red. This figure also illustrates that there are multiple deviation routes available around the widely spaced convective elements. Figure 14 shows that the number of flashes accumulated at each EDR position increases as the aircraft measured turbulence increases indicating that the positions with the most lightning flashes are also the same positions in which the aircraft is most at risk for turbulence. For example, positions 8 and 9 feature 44 and 74 flashes which correspond with turbulence of 0.18 and 0.26 respectively. Similarly, Figure 15 shows a general trend of decreasing spatial separation between the position and the nearest lightning initiation being inversely correlated with increases in aircraft turbulence. As in the previous example, positions 8 and 9 indicate minimum distance to flashes of 7 and 1 nmi with turbulence of 0.18 and 0.26 in these positions. These plots illustrate that the amount of and distance to lightning initiations from EDR positions are directly related to the turbulence threat in those areas.

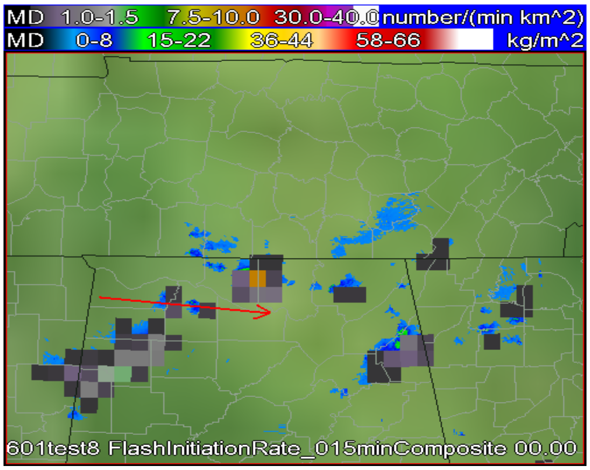

Figure 13: Flash initiation density (black squares) and WSR-88D VIL and aircraft track (red).

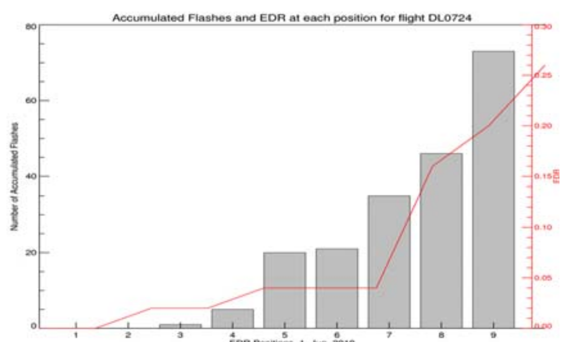

Figure 14: Accumulated flashes at each EDR report position for the duration of DL0724 (bars) and aircraft EDR turbulence (red).

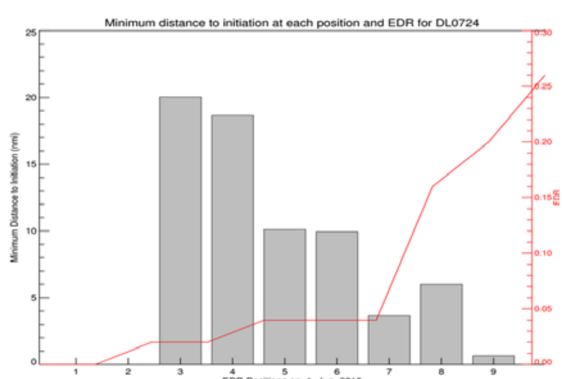

Figure 15: Minimum distance to LMA flash initiations (bars) at each position for the duration of DL0724 and aircraft EDR turbulence (red) measured along flight path.

6. CONCLUSIONS

From the results shown above it is apparent that the inclusion of total lightning data along with other remote sensing data can result in improved identification and subsequent avoidance of convection.

Adding total lightning information to general plots of radar variables like reflectivity and VIL can help to highlight areas that may not stand out in radar data alone, as was the case for DL2007 in late January of 2010. Total lightning information helped to identify which cells were the most robust in a generally uniform convective scene from a radar perspective. Our results also show that there was general agreement between the total lightning trends identified by LMA, GLM proxy, and ENTLN suggesting that the results found in this study should be applicable across a wider region than can be covered by a single LMA network, whether it be from a ground-based network like ENTLN or from a space-based platform such as GLM. Airline dispatchers and pilots could certainly benefit from total lightning data on the wide spatial extent offered by a geostationary total lightning detector. Our results showed that a flash initiation density product from GLM could serve to identify the more dangerous cells in a convective environment and in cases where radar coverage is poor or unavailable, total lightning information from the GLM could stand alone as a thunderstorm detector and CIT avoidance tool.

The use of spatial information contained in EDR turbulence data allowed us to examine the total number of flashes and the minimum distance to flashes within 20 nmi of those positions regardless of whether the aircraft was currently occupying them. This technique could easily be modified to examine lightning information along a predetermined flight plan to highlight exactly which areas along the flight path are experiencing more and closer flashes and have an increased likelihood of CIT encounters. Data of this nature could inform pilots and aircraft dispatchers of upcoming dangerous regions before the choice to deviate from a predetermined flight plan is more costly in terms of both fuel expenditure and aircraft safety.

7. REFERENCES

Bateman, M. D. Mach, E. W. McCaul, J. Bailey, and H. J. Christian, 2008: A comparison of lightning flashes as observed by the lightning imaging sensor and the North

Alabama lightning mapping array. *Third Conference on Meteorological Applications of Lightning Data*. New Orleans, LA, Amer. Meteor. Soc., **8.6**.

Bedka, K., J. Brunner, R. Dworak, W. Feltz, J. Otkin, and T. Greenwald, 2010: Objective satellite-based detection of overshooting tops using infrared window channel brightness temperature gradients. *J. Appl. Meteor. Climatol.*, **49**, 181–202.

Cornman, L. B., and B. Carmichael, 1993: Varied research efforts are under way to find means of avoiding air turbulence. *ICAO J.*, **48**, 10–15.

Cornman, L.B., C. S. Morse, and G. Cunning, 1995: Real-time estimation of atmospheric turbulence severity from in-situ aircraft measurements. *J. Aircr*., **32**, 171–177.

Cummins, K. L., M. J. Murphy, E. A. Bardo, W. L. Hiscox, R. B. Pyle, and A. E. Pifer, 1998: A combined TOA/MDF technology upgrade of the U.S. National Lightning Detection Network. *J. Geophys. Res.,* **103,** 9035–9044.

Deierling, W., and W. A. Petersen, 2008: Total lightning activity as an indicator of updraft characteristics. *J. Geophys. Res*., **113**, D16210, doi:10.1029/2007JD009598.

Federal Aviation Administration, 2012: Chapter 7. FAA Aeronautical Information Manual. [Available online at www.faa.gov/air_traffic/publications/atpubs/aim.]

Goodman, S. J., D. E. Buechler, P. D. Wright, and W. D. Rust, 1988: Lightning and precipitation history of a microburst-producing storm. *Geophys. Res. Lett*., **15**, 1185-1188.

_____, S. J. and Coauthors, 2005: The North Alabama Lightning Mapping Array: Recent severe storm observations and future prospects. *Atmos. Res*., 76, 423-437.

Hamilton, D. W., and F. H. Proctor, 2006b: Progress in the development of an airborne turbulence detection system. Preprints, *12th Conf. on Aviation, Range, and Aerospace Meteorology,* Atlanta, GA, Amer. Meteor. Soc., P6.5. [Available online at http://ams.confex.com/ams/pdfpapers/104475.pdf.].

Kaplan, M. L., A. W. Huffman, K. M. Lux, J. J. Charney, A. J. Riordan, and Y.-L. Lin, 2005: Characterizing the severe turbulence environments associated with commercial aviation accidents. Part 1: A 44-case study synoptic observational analyses. *Meteor. Atmos. Phys.,* **88,** 129–152.

Koshak, W. J. and Coauthors, 2004: North Alabama Lightning Mapping Array (LMA): VHF source retrieval algorithm and error analysis. *J. Atmos. Ocean. Tech*., **21**, 543-558.

Lane, T. P., R. D. Sharman, T. L. Clark, and H. M. Hsu, 2003: An investigation of turbulence generation mechanisms above deep convection. *J. Atmos. Sci*., **60**, 1297–1321.

_____, T. P., R. D. Sharman, S. B. Trier, R. G. Fovell, and J. K. Williams, 2012: Recent advances in the understanding of near-cloud turbulence. *Bull. Amer. Meteor. Soc*., **93**, 499–515.

Liu, C. and S. Heckman, 2010: The Application of Total Lightning Detection and Cell Tracking for Severe Weather Prediction. *TECO-2010-WMO Technical Conference on Meteorological and Environmental Instruments and Methods of Observation*, Helsinki, Finland, 10 pp.

McCaul, E. W., J. Bailey, S. J. Goodman, R. Blakeslee, and D. E. Buechler, 2005: A flash clustering algorithm for North Alabama Lightning Mapping Array data. *Preprints, Conf. on Meteorological Applications of Lightning Data*, San Diego, CA, Amer. Meteor. Soc., CD-ROM, 5.2.

_____, E. W., S. J. Goodman, K. M. LaCasse, and D. J. Cecil, 2009: Forecasting lightning threat using cloud-resolving model simulations. *Wea. Forecasting*, **24**, 709–729.

Proch, D.A., 2010: Assessment of Lightning Jump Algorithms Using GOES-R GLM-Proxy Data for Severe Weather Detection. M.S. Thesis, University of Alabama-Huntsville, 64 pp.

Rison, W., R. J. Thomas, P. R. Krehbiel, T. Hamlin, and J. Harlin, 1999: A GPS-based three dimensional lightning mapping system: Initial observations in central New Mexico. *Geophys. Res. Lett.*, **26**, 3573-3576.

Schultz, C. J., W. A. Petersen, and L. D. Carey, 2011: Lightning and severe weather: A comparison between total and cloud-to-ground lighting trends. *Wea. Forecasting*, **26**, 744–755.

Steiger, S. M., R. E. Orville, and L. D. Carey, 2007: Total lightning signatures of thunderstorm intensity over North Texas. Part I: Supercells. *Mon. Wea. Rev.*, **135**, 3281-3302.

Thompson, K.B., 2013: A Comparison of Two Ground-Based Lightning Detection Networks against the Satellite-Based Lightning Imaging Sensor (LIS). M.S. Thesis, University of Alabama-Huntsville, 330 pp.

Weber, M. E., J. Evans, M. Wolfson, R. DeLaura, B. Moser, B. Martin, J. Welch, J. Andrews, and D. Bertsimas, 2006: Improving air traffic management during thunderstorms. 12th *Conference on Aviation Range and Aerospace Meteorology*, Atlanta, GA, Amer. Meteor. Soc., **10.3**.

Wiens, K. C., S. A. Rutledge, and S. A. Tessendorf, 2005: The 29 June 2000 supercell observed during steps. Part II: Lightning and charge structure. *J. Atmos. Sci.*, **62**, 4151-4177.

Williams, E. R. and Coauthors, 1999: The behavior of total lightning activity in severe Florida thunderstorms. *Atmos. Res.*, **51**, 245-265.